Food Chemistry 352 (2021) 129354

Contents lists available at ScienceDirect

Food Chemistry

journal homepage: www.elsevier.com/locate/foodchem

Visible on-site detection of Ara h 1 by the switchable-linker-mediated precipitation of gold nanoparticles

Eunghee Kim [a,1], Jungwoo Hahn [b,1], Choongjin Ban [d], Youngje Jo [e], Hyebin Han [a], Seokwon Lim [f,*], Young Jin Choi [a,b,c,*]

[a] Department of Agricultural Biotechnology, Seoul National University, 1 Gwanakro, Gwanakgu, Seoul 08826, Republic of Korea
[b] Center for Food and Bioconvergence, Seoul National University, 1 Gwanakro, Gwanakgu, Seoul 08826, Republic of Korea
[c] Research Institute for Agriculture and Life Sciences, Seoul National University, 1 Gwanakro, Gwanakgu, Seoul 08826, Republic of Korea
[d] Department of Environmental Horticulture, University of Seoul, 163 Seoulsiripdaero, Dongdaemun-gu, Seoul 02504, Republic of Korea
[e] Crop Post-harvest Technology Division, Department of Central Area Crop Science, National Institute of Crop Science, Rural Development Administration, Suwon 16429, Republic of Korea
[f] Department of Food Science and Biotechnology, College of BioNano Technology, Gachon University, Seongnam-Si, Gyeonggi-Do 13120, Republic of Korea

ARTICLE INFO

Keywords:
Ara h 1
Visible on-site detection
Switchable linker (SL)
Precipitation of gold nanoparticles (AuNP)

ABSTRACT

Biosensors have been widely applied in tests for allergens, but on-site detection remains a challenge. Herein, we proposed a detection procedure for peanut Ara h 1 as a representative allergen, which was extracted from a cookie, thereby minimising the need for any complex pretreatment that was difficult to perform, and enabling the visual detection of the target without the use of analytical equipment. The extraction procedure was performed in less than 30 min using a syringe and filter (0.45 μm). The detection method for Ara h 1 was based on the aggregation of switchable linkers (SL) and gold nanoparticles (AuNP), and the presence of 0.19 mg peanut protein per 30 g of cookie could be confirmed within 30 min based on the AuNP/SL concentration ratio by the precipitation. This proposed procedure could be successfully applied to the detection of a wide range of food allergens.

1. Introduction

Food allergies are a significant issue worldwide for both food industries and public health. Because no effective cure has been developed for food allergies, avoidance of foods containing allergen(s) is the most appropriate way to prevent reactions or problems (Du Toit, Sampson, Plaut, Burks, Akdis, & Lack, 2018). For this reason, many countries have established regulations for labelling allergenic ingredients in prepackaged foods (Rizzi, Zoccatelli, Simonato, Fratea, & Mainente, 2017; Shoji, Adachi, & Akiyama, 2018), and many food manufacturers voluntarily perform precautionary allergen labelling (PAL) (Allen et al., 2014; Crotty & Taylor, 2010; Remington, Baumert, Blom, Houben, Taylor, & Kruizinga, 2015). However, these warnings are often ignored by consumers due to mislabelled PAL that are not based on a quantitative allergen risk assessment (Zhang, Hong, Cai, Huang, Wang, & Ren, 2019). Therefore, it is essential to engage the public in the analysis of food allergens by developing consumer-friendly detection methods. Seventy-five percent of peanut-allergic individuals are reported to have serum-specific IgE against the peanut protein 7S globulin (Ara h 1), which accounts for 12–16% of peanut protein (Goliáš, Humlová, Halada, Hábová, Janatková, & Tučková, 2013). Ara h 1 is composed of a stable homo-trimer that is bound by hydrophobic interactions between residues in the α-helical bundles of 63.5 kDa monomers (Burks, Cockrell, Stanley, Helm, & Bannon, 1995; van Boxtel, van Beers, Koppelman, van den Broek, & Gruppen, 2006). Therefore, Ara h 1, which has a stable structure, is widely used as a representative allergen marker (Palladino & Breiteneder, 2018).

In recent decades, many effective techniques have been extensively applied to ensure the proper labelling and management of food allergens, including Ara h 1. These techniques include the enzyme-linked

* Corresponding authors at: Department of Food Science and Biotechnology, College of BioNano Technology, Gachon University, Seongnam-Si, Gyeonggi-Do 13120, Republic of Korea (S. Lim); Department of Agricultural Biotechnology, Seoul National University, 1 Gwanakro, Gwanakgu, Seoul 08826, Republic of Korea (Y. J. Choi).
E-mail addresses: slim@gachon.ac.kr (S. Lim), choiyj@snu.ac.kr (Y.J. Choi).
[1] Co-first authors.

https://doi.org/10.1016/j.foodchem.2021.129354
Received 29 July 2020; Received in revised form 17 January 2021; Accepted 9 February 2021
Available online 20 February 2021

immunosorbent assay (ELISA) (Jayasena, Koppelman, Nayak, Taylor, & Baumert, 2019; Montserrat et al., 2015), reverse-phase high-performance chromatography (RP-HPLC) (Singh, Cantoria, Malave, Saputra, & Maleki, 2016), surface enhanced Raman spectroscopy (Gezer, Liu, & Kokini, 2016), magneto-resistive (Ng, Nadeau, & Wang, 2016), electrochemical sensors (Sobhan, Oh, Park, Kim, Park, & Lee, 2018), DNA-based sensors (Zhang, Wu, Wu, Ping, & Wu, 2019)), real-time polymerase chain reaction (PCR) (Miyazaki et al., 2019; Puente-Lelievre & Eischeid, 2018) and the loop-mediated isothermal amplification (LAMP) (Sheu, Tsou, Lien, & Lee, 2018). Despite these many methods, a need remains for the development of on-site detection methods that can be used without time-consuming preparation, trained experts and/or sophisticated instruments.

In this paper, our aim was to provide a simple and fast method for the on-site detection of Ara h 1 as a model allergen target based on our developed gold nanoparticle (AuNP)-precipitation-based detection system (Hahn, Kim, Han, & Choi, 2020; Hahn, Kim, You, Gunasekaran, Lim, & Choi, 2017; Lim et al., 2012; You, Lim, Hahn, Choi, & Gunasekaran, 2018). This technique generates a visible signal with the precipitation of aggregates of AuNP and the target protein. A key element in determining the aggregate size is the switchable linker (SL), with the precipitation of aggregates generated by changing the ratio of AuNP to SL, thereby enabling quantitative detection of the target. This detection method includes a simple extraction process using an easy-to-use syringe filter and a AuNP precipitation analysis method suitable for field use. To evaluate the practical detection limit and quantification of Ara h 1, the proposed analytical method is performed with reference to the analytical sensitivity threshold recommended by the Voluntary Incidental Trace Allergen Labelling (VITAL 3.0) system (Bureau, 2019; Holzhauser et al., 2020). In addition, the developed method can evaluate selectivity based on excellent visible signals. Taken together, the results obtained by this proposed method demonstrate its practicality and simplicity in the detection of Ara h 1 in foods.

2. Experimental section

2.1. Materials

Chloroauric acid and bovine serum albumin (BSA) were purchased from Sigma Aldrich (St. Louis, MO, USA). Tri-sodium citrate was purchased from Yakuri Pure Chemicals Co., Ltd (Kyoto, Japan). Tetraborate pH standard solution was purchased from Wako Pure Chemicals Industries, Ltd (Osaka, Japan). Phosphate-buffered saline (PBS) was purchased from Thermo Fisher Scientific (Waltham, MA, USA). Thiolated streptavidin was purchased from Protein Mods (Madison, WI, USA). Purified natural Ara h 1, biotinylated monoclonal anti-Ara h 1 IgG1 (clone 2F7 C12 D10) antibody, and Ara h 1 ELISA kit EL-AH1, which contains mouse monoclonal IgG1 (2C12) and biotinylated mouse monoclonal IgG1 (2F7), were purchased from Indoor Biotechnologies (Cardiff, UK). The method used by the ELISA kit to detect Ara h 1 is included in the supplementary information. The filter (0.45-μm pore size) was purchased from Milipore (Billerica, MA, USA). Roasted peanuts, tree nuts (almonds, cashew nuts, hazelnuts, pecans, and walnuts), and legumes (black-eyed peas and soybeans) were purchased from Lotte, Ltd (Seoul, Korea). Skippy creamy peanut butter were purchased from Hormel Foods, LLC (Austin, MN, USA).

2.2. Instrumentation

Absorbance measurements were performed on a UV-1700 spectrophotometer (Shimadzu, Kyoto, Japan). The pH values of all buffer solutions were determined using the Professional Meter PP-15 (Satorious, Göttingen, Germany). Particle sizes and distributions were determined by dynamic light scattering (DLS) with a Zetasizer Nano-ZS 90 (Malvern, Worcestershire, UK). Transmission electron microscopic (TEM) images were obtained using a LIBRA 120 transmission electron microscope (Karl Zeiss, Oberkochen, Germany).

2.3. Preparation of gold nanoparticles (AuNP)

Gold nanoparticles (AuNP) 30.0 ± 0.5 nm in diameter were synthesised according to the method established by Bastus et al. (Bastús, Comenge, & Puntes, 2011). Briefly, 150 mL of sodium citrate solution (2.2 mM) was brought to boiling. Once boiling had begun, 1 mL of chloroauric acid ($HAuCl_4$) solution (25 mM) was added to the boiling solution. When the colour of the solution had changed to soft pink, the solution was cooled to 90 °C in a water bath, and the cooled solution was used as a seed solution for the growth process. To grow the AuNP, 1 mL of $HAuCl_4$ solution (25 mM) was added to the seed solution twice at 30-min intervals. After the reaction was finished, 55 mL of the sample was extracted. The remaining sample was then diluted by adding 55 mL of a sodium citrate solution (2.2 mM). After the temperature of the diluted solution had returned to 90 °C, the growth process was repeated using the diluted solution as the seed solution. This process was repeated three times. Ultimately, AuNP 30 nm in diameter were obtained and stored at 4 °C until further use. The particle sizes of the AuNP were determined using an ultraviolet/visible (UV/Vis) spectrophotometer and DLS.

2.4. Preparation of streptavidin-coated gold nanoparticles (stAuNP)

Six hundred microliters of AuNP (absorbance of 4.0 at 526.0 ± 0.5 nm, diameter of 30 nm) were incubated with 100 μL of BSA (100 μg/mL) in borate buffer (pH 7.4) for 30 min. After incubation, the mixture was reacted with 100 μL of thiolated streptavidin (50 μg/mL) in borate buffer (pH 7.4) for 30 min. Unbound streptavidin was removed by repeated centrifugation (relative centrifugal force, 5000, 30 min), and pellets of streptavidin-coated AuNP (stAuNP) were resuspended in PBS 1× (pH 7.4) containing 0.05% (w/v) BSA. The concentration was then adjusted to an absorbance of 6.0 at 536.0 ± 0.5 nm (Fig. S1B). This concentration of AuNP in solution was estimated based on the absorbance value as ~1.19×10^{12} particles per mL. The additional physicochemical analysis of the surface modification of the AuNP used in this study is shown in Fig. S1 and detailed in Table S1.

We controlled the degree of coating of streptavidin by first coating BSA on the AuNP and then coating streptavidin on the empty spaces remaining on the surfaces of the AuNP. The tetrameric structure of streptavidin can induce aggregation of AuNP, whereas the stable monomeric structure of BSA does not.

2.5. Detection of Ara h 1 in standard solution

The detection system comprised two steps. In the first step, 100 μL of standard Ara h 1 solution (0, 25 ng/mL, 250 ng/mL, 2.5 μg/mL, 5.0 μg/mL and 10.0 μg/mL), which was a part of the purchased ELISA kit, was mixed with biotinylated anti-Ara h1 antibody (b-Ab) in concentrations ranging from 0.5 μg/mL to 0.9 μg/mL. The mixture was then mildly agitated for 15 min. In the second step, 200 μL of stAuNP (absorbance of 6.0 at 536.0 ± 0.5 nm) was added and then agitated for an additional 15 min. The shift in the range exhibiting a visible colour change, which is referred to as the REVC, was identified visually and/or by UV/Vis spectroscopy in the 400–700 nm range. A standard Ara h 1 solution was prepared by diluting purchased Ara h 1 in PBS 1× (pH 7.4).

2.6. Preparation of model cookies for a detection experiment on a real matrix

For use in a real-sample detection experiment, sample cookies were prepared using the following procedure. The cookie ingredients were purchased at a local market. Eighty grams of brown sugar (CJ CheilJedang, Incheon, South Korea) and 0.5 g of salt (Taepyung Salt Co., Shinan, South Korea) were mixed into and dissolved in 80 g of melted butter (Lotte Food, Cheonan, South Korea). One egg (Tetgol Farm Co.,

Youngin, South Korea) and 1 g of pure vanilla extract (Lorannoils INC., MI, USA) were added and uniformly mixed into the blended butter solution to obtain a premix. Dry ingredients, including 150 g of wheat flour (CJ CheilJedang, Yangsan, South Korea) and 1 g of baking soda (Bread Garden, Seongnam, South Korea), were then combined with the premix. To produce a model cookie, roasted peanuts (Qingdao Jiaoping Foods Co., Qingdao, China) were ground into powder in a blade-mixer (SFM-500SP, Shin-Il, South Korea) and 0.0025 wt%, 0.025 wt%, 0.5 wt%, 1 wt%, and 5 wt% of powdered peanut were mixed into each premix. The fully homogenised dough was divided into 30-g portions for each sample to ensure that the cookies were of the same size. The cookies were baked in a light-wave oven (KAO-H013, KitchenArt, South Korea) for 20 min at 180 °C.

2.7. Detection of Ara h 1 in cookie extract solution

Sample extracts were prepared according to previously described procedures (Walczyk, Smith, Tovey, & Roberts, 2017) with minor modifications. Briefly, 30 g of the sample was ground and dissolved into 300 mL of 20 mM Tris-HCl buffer (pH 8.5), which was then agitated for 15 min at room temperature. The extracts were filtered through a 0.45-μm syringe filter to remove solid debris. The filtered cookie extract solutions were diluted 10-fold with PBS 1x (pH 7.4) and then mixed with b-Ab ranging in concentrations from 0.5 μg/mL to 0.9 μg/mL. The remaining steps were performed in the manner described above. The Ara h 1 concentration in the cookie extract solution was measured using the commercial ELISA kit.

2.8. Verification of the selectivity of the detection method

Cookie samples containing 5.0 wt% tree nuts (almond, cashew nut, hazelnut, pecan, and walnut) and legumes (soybean, and black-eyed pea) were used in the selectivity tests. Each sample extract solution was diluted 10-fold with PBS 1x (pH 7.4) and then mixed with b-Ab ranging in concentrations from 0.5 μg/mL, 0.7 μg/mL and 0.9 μg/mL. The remaining steps were performed in the manner described above.

2.9. Statistical analysis

The data represent an average of at least three independent experiments or measurements, and the results are expressed as mean ± standard deviation (SD).

3. Result and discussion

3.1. Overall detection procedures

In this study, we focused on a detection process that could be used when on-site detection was required. We propose an easy and quick detection procedure that involves simple extraction and minimal pretreatment. Fig. 2 shows a schematic of the on-site detection procedure for Ara h 1 as a representative food allergen. This procedure enables Ara h 1 to be quickly, accurately, and sensitively detected in a real cookie using a simple device. First, the prepared model cookie can be easily crushed by hand and powdered for extraction. To realize short and simple extraction, the procedure is designed to perform extractions within 15 min at room temperature using Tris-HCl buffer (pH 8.5). The procedure consists of dissolution and purification steps. First, the crushed cookie is dissolved in Tris-HCl buffer for approximately 15 min, and then the extract is filtered through a readily available commercial 50-mL syringe and syringe filter (pore size 0.45 μm) to remove solid debris. Using this procedure, Ara h 1 can be extracted quickly and simply from cookies in the field. After simple extraction, the solution containing the target Ara h 1 is easily tested by the proposed detection system based on SL-induced AuNP precipitation. This method is also designed specifically for field applications and requires no washing or complicated probe immobilisation procedures. In addition, the detection results can be visually read by the naked eye. To apply this procedure in the field problems such as automation, simplification, and miniaturisation of sample preparation and detection must be addressed, but the proposed detection procedure is considered to be a significant step toward on-site applications.

3.2. Hypothesised mechanism for Ara h 1 detection

As shown in Fig. 1, the proposed method consists of a control line without a target and a test line with a target, and is designed to involve two sequential steps: (1) reaction of the SL (b-Ab) and the target (Ara h 1), i.e., the target recognition step, and (2) after the reaction time has elapsed, the addition of functionalised AuNP (stAuNP), i.e., the signal indication step. Two regions can be distinguished in the AuNP/SL aggregates: the REVC with colour change and the region with no colour change (in which the number of linkers that could react with the particles was insufficient or the binding site of the particles were already filled by the linker). The REVC of the control line was determined by the quantitative relationship between the AuNP and SL. In the test line with the target, the SL can be switched off as the SL binds to Ara h 1, which shifts the REVC to a higher linker concentration range than that of the control line. This colour difference can be used to quantitatively detect the target.

The hypothesised detection mechanism is shown in Fig. 1, which is based on the change in the aggregation pattern according to the quantitative correlations among the SL, targets, and AuNP. The SL is an aggregation mediator that can form aggregates with both the targets and AuNP. When the AuNP and SL react at a specific ratio, they form large aggregates, which causes fast precipitation. However, if the target in the sample is preferentially recognised, an SL/target aggregate can form. The resulting aggregate interferes with the formation of AuNP and SL aggregates, which leads to a change in the optimum AuNP/SL ratio for rapid precipitation. Alteration in the precipitation rate of the AuNP/SL aggregates provokes a shift in the visible colour change (REVC) and absorbance in the solution containing them.

The SL used in this study was a crosslinking agent that recognises targets in addition to inducing the large-scale aggregation (aggregates can be precipitated) of AuNP. The SL can induce large-scale aggregations when a specific concentration ratio with AuNP is realized. In addition, when the SL is switched off by a specific target such as Ara h 1, this specific concentration ratio is readjusted to change the extent of the large-scale aggregation. Unlike colour changes, such as the red and/or blue shift in other colorimetric assays, the colorimetric signal generated by the precipitation of aggregates is more intuitive because the large-scale aggregation reduces the dispersion of AuNP in the system, such that the colour disappears.

The two-step reaction of this system clearly shows the difference in susceptibility between the Ara h 1-antibody interaction in the signal indication step and the streptavidin–biotin binding in the target recognition step. In the Ara h 1–antibody and streptavidin–biotin cases, the equilibrium dissociation constants (K_D) are known to be roughly 10^{-12} M^{-1} and 10^{-15} M^{-1}, respectively (Chivers, Crozat, Chu, Moy, Sherratt, & Howarth, 2010; Huang, Bell, & Suni, 2008). However, the difference in the dynamics of these two reactions do not affect the operation of the system, which can be readily explained. First, the system consists of two independent sequential steps (the Ara h 1–antibody interaction in the target recognition step and the streptavidin–biotin binding in the signal indication steps). Second, each reaction occurs at a different binding site and has a minimal effect on the other reaction. The reactions are not competitive. Third, the streptavidin/biotin reaction occurs much more rapidly than the Ara h 1/antibody reaction, which results in the rapid formation of large-scale aggregates of AuNP with the SL. These large-scale aggregates then precipitate by gravity depending on their size, which results in a visual signal. In this situation, even if the SL is switched on by the reverse reaction of Ara h 1/Ab (such as the SL being

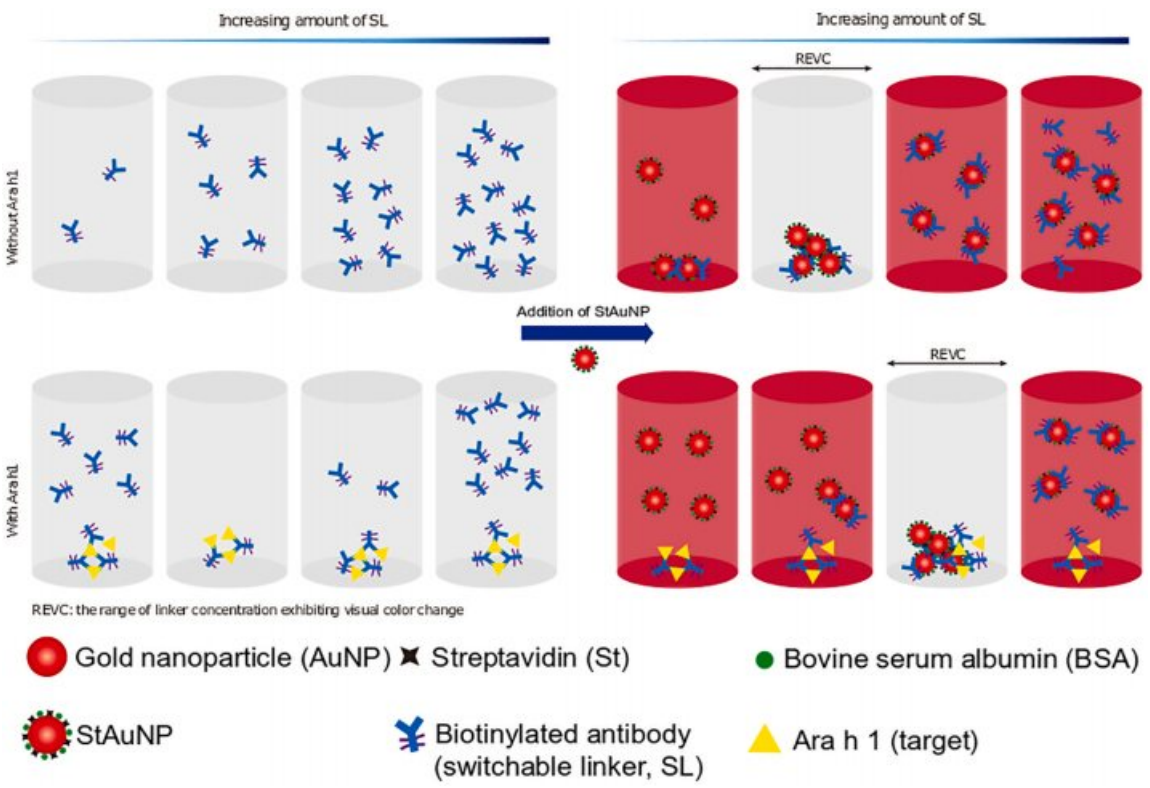

Fig. 1. Schematic of the colorimetric and visual detection of Ara h 1 based on the shift in the range of the exhibiting visible colour change (REVC). First, biotinylated Ara h 1 antibody (the SL) was added to solutions with or without the target (Ara h 1). Then, streptavidin-coated gold nanoparticles (stAuNP) were added to the solutions. The target decreased the aggregation capacity of the SL, which caused the AuNP to form an optimal aggregation with a higher SL concentration than that without the target.

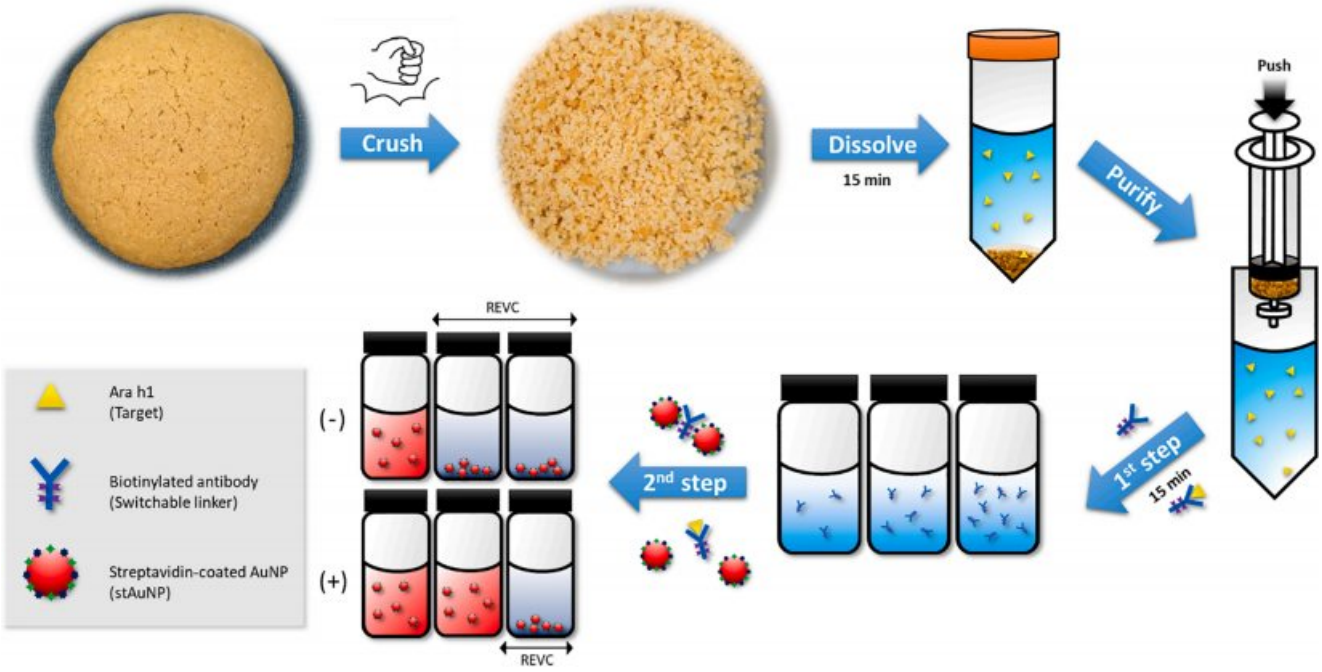

Fig. 2. Schematic of overall detection procedures, including peanut extraction and Ara h 1 detection.

detached from the Ara h 1), it has little chance of reacting with the aggregates. This process occurs because the larger are the aggregates, the relatively slower is the reaction rate. Gold nanoparticles that do not participate in the formation of aggregates can bind with the switched-on SL, but this process would generate only relatively small-scale aggregates that cannot be precipitated and would be very unlikely to affect the REVC. For these reasons, we believe that the reversibility issue has minimal impact on the sensitivity. In addition, there are some samples

for which precipitation occurs slowly depending on the size of the aggregates after the detection time we set (30 min), but this is unrelated to the reversibility.

3.3. Detection of Ara h 1 in PBS using the proposed method

Before on-site application, this detection strategy must be optimised in terms of the Ara h 1-induced REVC shift that is influenced by the concentrations/ratios of b-Ab and stAuNP. To do so, first, we determined the REVC signal of the control (no target), as shown in Fig. S2. This REVC signal was observed at b-Ab concentrations ranging from 0.5 μg/mL to 5.0 μg/mL. A clear precipitate among the stAuNP and b-Ab was observed at b-Ab concentrations ranging from 1.0 μg/mL to 2.0 μg/mL, whereas only a slight colour difference (purplish red) was observed at concentrations of 0.5 μg/mL (low end) and 3.0 μg/mL (high end). This colour difference can be mainly attributed to the surface plasmon resonance (SPR) difference due to the presence of small stAuNP-*b*-Ab aggregates that had not yet precipitated. In the treatment of Ara h 1 (10.0 μg/mL and 20.0 μg/mL in Fig. S2), a right-side REVC shift, as compared with the control REVC, was observed in the b-Ab concentration ranges of 1.0–4.0 μg/mL and 1.0–5.0 μg/mL, respectively. Then, we further subdivided the b-Ab concentration ranges used for the Ara h 1 detection to obtain a finer and more sensitive quantitative signal change (for example, the REVC shift), from which we determined the b-Ab concentration range to be 0.5–0.9 μg/mL (Ara h 1, 2.5–10.0 μg/mL). As shown in Fig. 3A, the REVC shift at the low end was clearly observed as the concentration of Ara h 1 was increased from 0 (control samples) to 10.0 μg/mL. When only b-Ab and stAuNP formed aggregates without Ara h 1 in the control samples, precipitation occurred at all concentrations, excepting the lowest b-Ab concentration of 0.5 μg/mL (the lowest in this experiment). However, the reaction of b-Ab with 2.5 μg of Ara h 1 showed no precipitation even at a concentration of 0.6 μg/mL (REVC shift occurred). As the amount of reacted Ara h 1 increased, the precipitation area (REVC) gradually shifted to higher SL concentrations. As shown in Fig. 3B and 3C, we identified the pattern of aggregate formation based on the presence or absence of Ara h 1 observed by TEM at 0.9 μg/mL of b-Ab. In the absence of Ara h 1, a large cluster several micrometers in size formed. In the presence of Ara h 1, however, aggregates among b-Ab, Ara h 1, and stAuNP were observed because they were not large enough to precipitate. It was easy to distinguish the precipitation area using the naked eye alone without the aid of an instrument.

To evaluate this strategy at the above SL concentrations, we used the ELISA method to detect and compare various concentrations of Ara h 1 (0, 2.5 μg/mL, 5.0 μg/mL, and 10.0 μg/mL) (Fig. 3A). With respect to the detection limit, using the proposed strategy and ELISA, we were able to detect Ara h 1 at the concentration of 250 ng/mL and 25.0 ng/mL, respectively (provided from Indoor Biotechnologies Inc.). In practice, the detection limit of the proposed method was more sensitive than that of the ELISA method, and the visual signal based on the REVC shift was easier to quantitatively confirm by the proposed method, as the ELISA method shows a colour change based on the colour density. In addition, the detection limit (25.0 ng) with enhanced visibility is considered to be meaningful because, to date, 0.19 mg of peanut protein has been generally required to induce an allergic reaction even in allergen-sensitised patients (Bureau, 2019). For these reasons, the proposed method is considered to be effective and practical for field applications.

According to the research of Remington et al. (2020), the eliciting doses (ED) for an allergic reaction in 1% and 5% of the population, known as ED01 and ED05, are estimated to be 0.2 mg and 2.0 mg of protein for peanuts, respectively. In addition, to confirm the sensitivity of the SL-based assay in a purified buffer at the ED01 and ED05 levels (0.19 mg of peanut protein or 25.0 ng of Ara h 1 and 1.9 mg of peanut protein or 250 ng of Ara h 1), biotinylated antibody concentrations were further subdivided into 0.600 μg/mL, 0.625 μg/mL, 0.650 μg/mL, 0.675 μg/mL, and 0.700 μg/mL. As shown in Fig. 3D, as the concentration of Ara h 1 increased, the REVC shifted to a higher linker concentration.

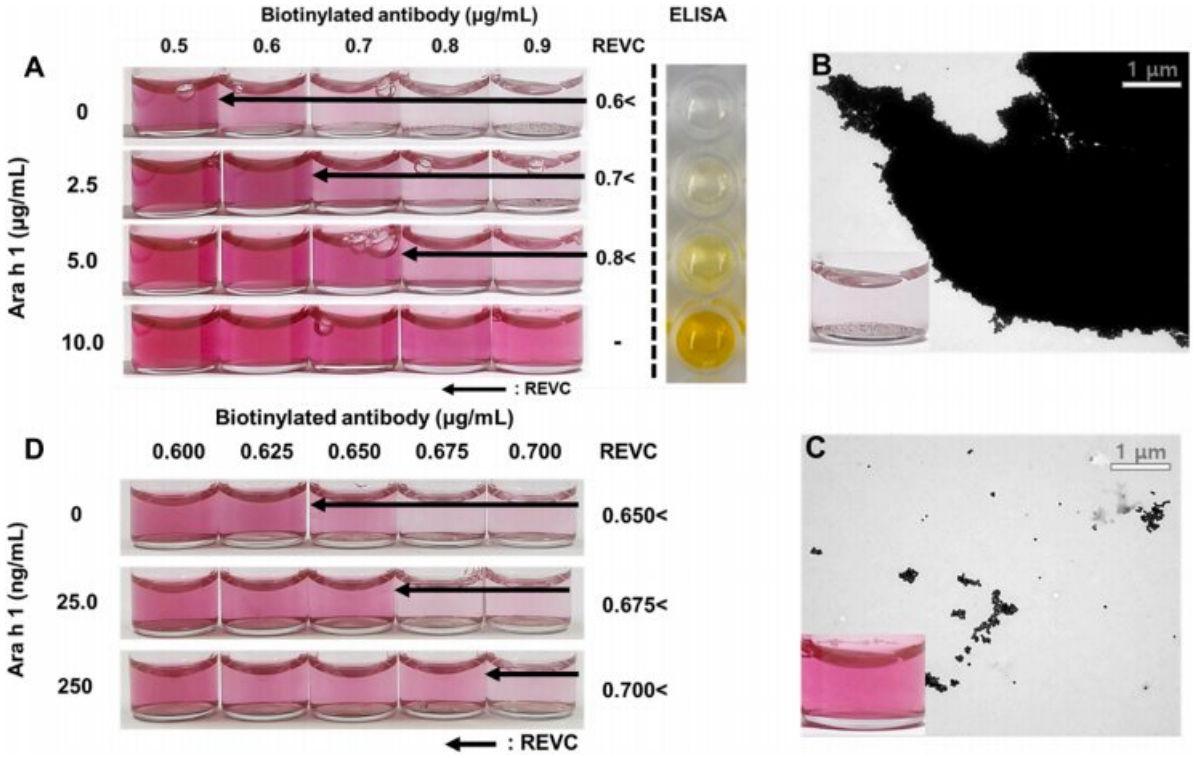

Fig. 3. (A) Detection of Ara h 1 (0.0, 2.5 μg/mL, 5.0 μg/mL, and 10.0 μg/mL) using the proposed switchable linker (SL)-based assay and the enzyme-linked immunosorbent assay (ELISA). Transmission electron micrographs of the Ara h 1-induced stAuNP aggregates (B, 0 μg/mL; C, 10.0 μg/mL) at 0.9 μg/mL of b-Ab (inset, photograph of their suspensions). (D) Detection of Ara h 1 (25.0 ng/mL and 250 ng/mL) using the proposed SL-based assay.

3.4. UV–vis spectroscopic approach to Ara h 1 detection

To quantify the visual signal and improve the detection limit of the proposed method, we used a spectrophotometer to analyse the change in absorbance of AuNP aggregates based on the previously mentioned mechanism. The ratio between the AuNP and SL was optimised by testing various concentrations, and finally we identified 0.7 μg/mL of SL, which is a low-end concentration of the control line in Fig. 3A, for use in the experiment. As shown in Fig. 3A, as the concentration of Ara h 1 was increased at a linker concentration of 0.7 μg/mL, the colour change was confirmed as being due to the precipitation of gold aggregates. To confirm the correlation between the colour change and the concentration of Ara h 1, the change in absorbance was measured. Several Ara h 1 solutions with concentrations between 0.125 μg/mL and 20.0 μg/mL (Fig. S3A) were tested. The changes in absorbance at a peak were found to be significant even with these small amounts of Ara h 1. We plotted the absorbance at 550 nm with the concentration of Ara h 1 to quantify the change in absorbance (Fig. S3B). The absorbances at 550 nm were found to be proportional to the concentrations of Ara h 1 in the range from 0.125 μg/mL to 4.00 μg/mL, which can be expressed as a linear equation:

$$A_{550\ \mathrm{nm}} = 0.0826 C_{\mathrm{Ara\ h\ 1}} + 0.1296\ (\mu\mathrm{g/mL}) \quad (1)$$

with a correlation coefficient of 0.9982 at $A_{550\ \mathrm{nm}}$ for absorbance at 550 nm and $C_{\mathrm{Ara\ h\ 1}}$ for the concentration of Ara h 1. The linear section (detection range) occurred from 0.125 μg/mL to 4.00 μg/mL, and the slope of the absorbance change decreased at higher concentrations (from 4.00 μg/mL to 20.0 μg/mL). Unlike the change in absorbance, almost no shift was observed in the SPR peak (about 2 nm shift) of the small molecule–target AuNP aggregation. Thus, little change in colour was observed. This finding is thought to be the result of interference by proteins of the plasmon interactions with AuNP, because proteins are relatively larger than AuNP (Sendroiu, Mertens, & Schiffrin, 2006). On the other hand, the speed and size of the AuNP/SL cluster formation were faster and larger than in the conventional AuNP aggregation-based detection method because of the number of biotin and streptavidin moieties, which can induce their aggregation on SL and stAuNP surfaces. Therefore, precipitation of the aggregates occurred within a short time (30 min), and the change in absorbance caused by this precipitation could be measured by a spectrophotometer.

Because AuNP induce colorimetric effects according to the localised surface plasmon resonance (LSPR) principle, nanoparticles in many studies have undergone changes in their size, shape, composition, and interparticle distance (C.-C. Huang, Huang, Cao, Tan, & Chang, 2005; Pavlov, Xiao, Shlyahovsky, & Willner, 2004). The interparticle distance of AuNP in this system was especially important for inducing the LSPR of AuNP. The AuNP (30 ± 0.5 nm) used in this system were coated with BSA (66.5 kDa, 5.45-nm hydrodynamics radius) and streptavidin (52.8 kDa, 4.9-nm hydrodynamic radius), and these coated AuNP (stAuNP) were designed to crosslink with each other via the SL (IgG1, 11.5-nm hydrodynamic radius) (Blanco, Via, Garcés, Madurga, & Mas, 2017; Mir, Maurya, Ali, Ubaid-Ullah, Khan, & Patel, 2014). Therefore, even if stAuNP-*b*-Ab aggregates had caused LSPR, the distance between the particles was relatively large, so no dramatic colour changes (red to blue) occurred. In conclusion, when small stAuNP/b-Ab aggregates were formed, their weak colour changes via SPR could have occurred with a small peak shift (2 nm), as shown in Fig. S3A.

3.5. Selectivity of the detection method

To determine the selectivity of the SL-based colorimetric detection system with respect to Ara h 1, we used the proposed method to test control samples (only PBS), peanut extracts, and seven other samples, including five tree nuts (almond, cashew nut, hazelnut, pecan, and walnut) and two legumes (black-eyed pea and soybean). To make the SL-based detection system more field-applicable and to identify the potential risk of this system of being inhibited by the potential factors of real foods, we conducted a selectivity experiment using real foods containing different allergen proteins. As shown in Fig. 4, the REVC of the peanut extract shifted and no precipitation occurred in the selected linker concentrations (from 0.5 μg/mL to 0.9 μg/mL). However, all the other extracts exhibited an REVC similar to that of the control sample. In addition, as shown in Fig. 4B, if we compare the absorbance of each sample at a 0.7-μg/mL linker concentration, the significant difference in the visual effect of the peanut test group compared to the other test groups is confirmed. The real food groups used in this experiment consisted of various components, including fat, protein, and minerals in addition to a pigment that could inhibit the colorimetric reaction of the AuNP. Therefore, good selectivity in the detection of targets in real foods is critical for detection strategies. Based on the results of this experiment, we confirm that the REVC of a system can be disturbed by the colour of the food itself in various food groups, including an almond, a cashew nut, or a black-eyed pea. However, having good selectivity with Ara h 1, this strategy clearly exhibits a colorimetric effect as an REVC if the appropriate linker concentrations (for example, 0.5 μg/mL and 0.9 μg/mL) are selected. Therefore, these results demonstrate that the proposed method has good selectivity and can be used for selective detection in mixed food samples.

It is very important to have good selectivity in the detection of a protein target in the extract of allergen-induced seed foods, because the extract contains a large number of soluble proteins, including 2S albumins (Costa et al., 2020), 7S globulins (vicilins) (Keum, Lee, & Oh, 2006), and 11S globulins (legumins) (Boualeg & Boutebba, 2017; Liu et al., 2007). In addition, as no series of pretreatment steps is performed, such as a washing process, this detection process by extraction requires good selectivity from a large number of proteins that may be similar to the target. Based on this experiment, the proposed method not only demonstrated that it can operate selectively for a variety of similar proteins but also confirmed that Ara h 1 can be detected via a simple extraction method. As such, this strategy is considered to be very effective for field applications.

3.6. Detection of Ara h 1 in model cookies

In this study, model cookies were prepared based on a one-piece serving (30 g), as established by the Food and Drug Administration (FDA) for the serving size of cookies. According to the VITAL® 3.0 reference dose, doses of 0.2 mg and 2.0 mg of peanut protein can trigger allergic reactions in 1% and 5% of the peanut-allergic population (ED01 and ED05), respectively. As peanuts have a conversion factor of four to allergenic food, less than 0.8 mg of peanuts can safely be included in food (Holzhauser et al., 2020). To determine the amounts of allowable peanut protein that satisfy the ED01 and ED05 safety criteria, cookies were made by mixing 0.75 mg and 7.5 mg of powdered peanut into each 30 g premix. These cookies had peanut protein contents equivalent to 0.19 mg and 1.9 mg, respectively, and 25.0 ng and 250 ng of Ara h 1 were detected in these same cookies. This amount of Ara h 1 corresponds to approximately 13.3% of total peanut protein, which is consistent with the previous study in which Ara h 1 accounts for 12–16% of the total peanut protein (Goliáš, Humlová, Halada, Hábová, Janatková, & Tučková, 2013). To evaluate the applicability of the proposed detection method to real samples, we detected estimated peanut-protein levels of 0.19 mg and 1.9 mg per 30 g of cookie (Fig. 5B) and 38 mg, 75 mg, and 750 mg per 30 g of cookie (Fig. 5A). As shown in Fig. 5A, the detection results exhibit a concentration-dependent shift in REVC. In the samples containing no peanut protein (control lines), precipitation as a visible signal occurred in the SL at concentrations above 0.5 μg/mL. As the concentration of peanut protein increased, the REVC shifted to higher SL concentration regions. As shown in Fig. 5B, we further subdivided the low-end region of the REVC, to determine the detection limit. The results showed a shift in the REVC down to a sample concentration of 0.19 mg

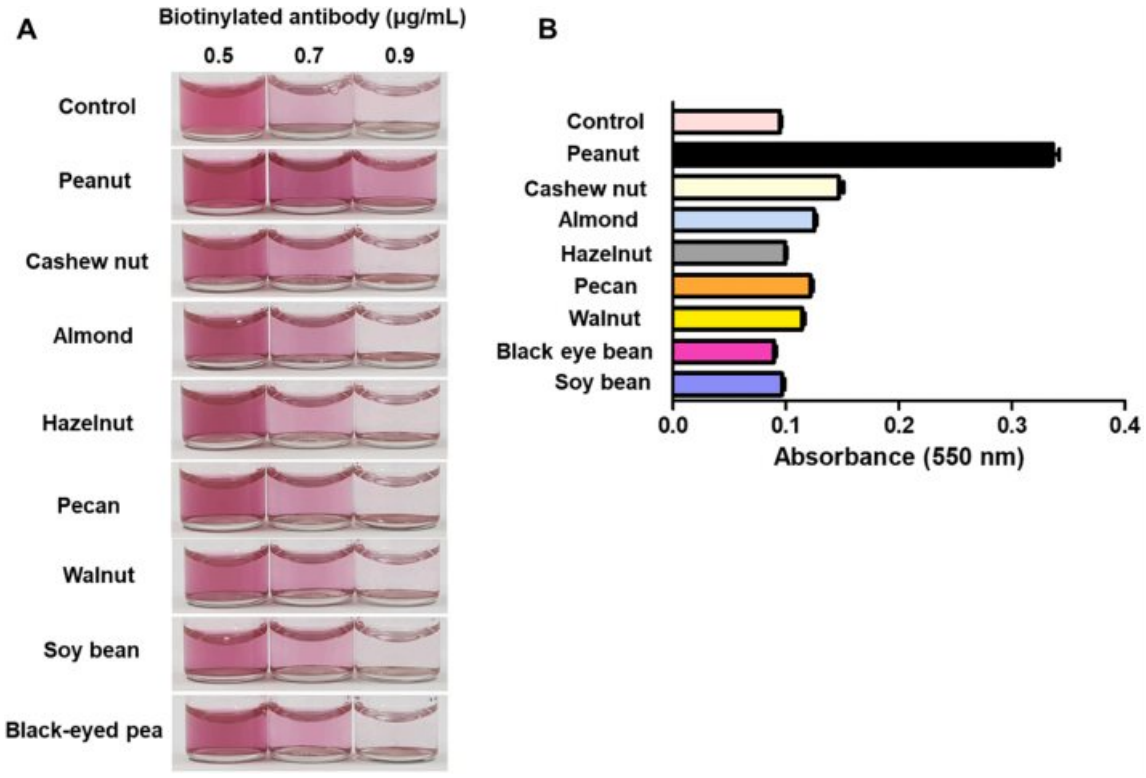

Fig. 4. Selectivity of the proposed SL-based colorimetric detection system. (A) The low-end REVC for detection with the solutions extracted from peanuts and several tree nuts (cashew nut, almond, hazelnut, pecan, and walnut) and legumes (soybean and black-eyed pea) (all extract solutions were diluted 10-fold with Tris-HCl buffer). (B) Comparison of absorbance at 550 nm of each sample with a biotinylated antibody concentration of 0.7 μg/mL. Control was a non-extract solution with Tris-HCl buffer.

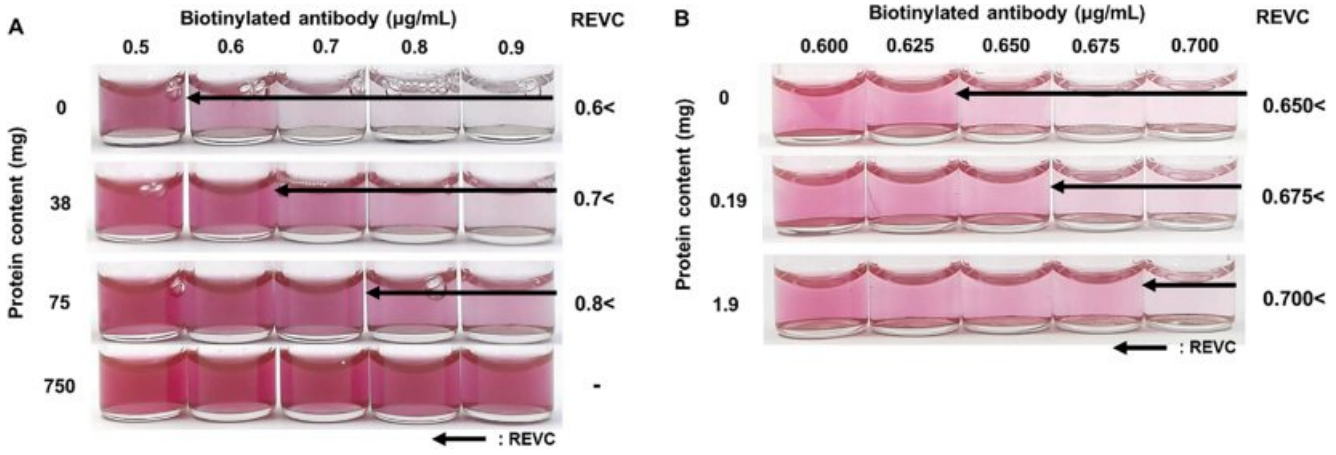

Fig. 5. Shift in the low-end REVC in response to the presence of Ara h 1 in cookie extract with 38 mg,75 mg, and 750 mg peanut protein (A) and 0.19 mg and 1.9 mg peanut protein (B) per 30 g of cookie.

of peanut protein per 30 g of cookie. These results indicate that the SL-based colorimetric detection method can detect peanut protein within 45 min to a concentration as low as 0.19 mg of peanut protein per 30 g of cookie, which satisfies ED01, and it exhibits the colorimetric effect (REVC shift) well without any inhibition even in real food. In addition, this result is significant in that the proposed detection process enables simple and fast field extraction of peanut protein and provides sensitive and convenient detection.

To validate the performance of our detection method, we compared our results with those obtained using a commercial ELISA method. Table 1 summarises the experimental results we obtained for an Ara h 1 standard solution spiked with 10 mg/mL of Ara h 1 and food samples

Table 1
Comparison of Ara h 1 detection in food samples using the enzyme-linked immunosorbent assay (ELISA) and the proposed method.

Samples	Concentration of Ara h 1(mg/mL)[a]		Recovery (%)
	ELISA method	Developed method	
Roasted peanut extract	3.43 ± 0.18	3.29 ± 0.28	95.9
Peanut butter extract	4.63 ± 0.31	4.59 ± 0.43	99.1
Ara h 1 standard solution	10.00 ± 0.32	10.66 ± 0.36	106.6

[a] Data are mean values of triplicate measurements. Values are shown as means ± standard deviation.

including roasted peanut extract and peanut butter extract. The recovery rates were 95.9%, 99.1%, and 106.6% of roasted peanut extract, peanut butter extract, and Ara h 1 standard solution, respectively. A *t*-test was also performed and the calculated concentrations obtained using the SL-based colorimetric detection method were not statistically different from those obtained using the ELISA method, with a 95% of confidence interval. These results strongly indicate that the proposed method can be applied to determine the presence of peanut protein in real samples. Furthermore, to evaluate the performance of the proposed detection method, Table S2 presents a comparison of our proposed method with other published methods for Ara h 1 detection. The SL-based assay was confirmed to show good sensitivity in the detection of peanut protein in real food samples without the use of any special device.

4. Conclusion

Anaphylaxis induced by food allergens is a major issue in many countries, including the US, as no clear method has been developed for treating food allergies. As such, there are active and ongoing studies to monitor the food allergens present in various foods in the field. In this study, we proposed a simple method for extracting Ara h 1 from food through a syringe and a simple and rapid method for detecting Ara h 1 based on SL-induced AuNP precipitation. The detection results indicate that aggregates composed of AuNP and SL at specific concentration ratios undergo rapid precipitation, and Ara h 1 can interfere with this aggregation, thus causing a change in the concentration ratio at which precipitation occurs. Within 45 min, we were able to determine Ara h 1 concentrations as low as 25.0 ng/mL with the naked eye. In addition, when measured by a UV/Vis spectrophotometer, we observed a linear absorbance change in the concentration range of 125–4,000 ng/mL. This detection method also worked well using a cookie extract of a real food matrix, showing a good detection limit (0.19 mg of peanut protein per 30 g of cookie) and good selectivity. Although problems such as the simplification and automation of detection must be solved for field applications, SL-based assays provide visibility of results, time efficiency, and ease-of-use that are suitable in the field while also representing a promising alternative for the detection of other allergens.

CRediT authorship contribution statement

Eunghee Kim: Conceptualization, Writing - original draft, Validation. **Jungwoo Hahn:** Methodology, Writing - review & editing, Funding acquisition. **Choongjin Ban:** Writing - review & editing. **Youngje Jo:** Investigation. **Hyebin Han:** Visualization. **Seokwon Lim:** Methodology, Funding acquisition, Supervision. **Young Jin Choi:** Methodology, Funding acquisition, Project administration, Supervision.

Declaration of Competing Interest

The authors declare that they have no known competing financial interests or personal relationships that could have appeared to influence the work reported in this paper.

Acknowledgement

This research was supported by the Basic Science Research Program through the National Research Foundation of Korea (NRF), which is funded by the Ministry of Education (2020R1F1A1074902, 2017R1D1A1B03028154 and 2020R1I1A1A01064445).

Appendix A. Supplementary data

Supplementary data to this article can be found online at https://doi.org/10.1016/j.foodchem.2021.129354.

References

Allen, K. J., Turner, P. J., Pawankar, R., Taylor, S., Sicherer, S., Lack, G., … Sampson, H. A. (2014). Precautionary labelling of foods for allergen content: Are we ready for a global framework? *World Allergy Organization Journal, 7*, 10. https://doi.org/10.1186/1939-4551-7-10.

Bastús, N. G., Comenge, J., & Puntes, Víctor (2011). Kinetically controlled seeded growth synthesis of citrate-stabilized gold nanoparticles of up to 200 nm: Size focusing versus Ostwald ripening. *Langmuir, 27*(17), 11098–11105.

Blanco, P. M., Via, M., Garcés, J. L., Madurga, S., & Mas, F. (2017). Brownian dynamics computational model of protein diffusion in crowded media with dextran macromolecules as obstacles. *Entropy, 19*(3), 105.

Boualeg, I., & Boutebba, A. (2017). Purification of water soluble proteins (2S albumins) extracted from peanut defatted flour and isolation of their isoforms by gel filtration and anion exchange chromatography. *Scientific Study & Research. Chemistry & Chemical Engineering, Biotechnology, Food Industry, 18*(2), 135.

Bureau, A. (2019). Summary of the 2019 VITAL Scientific Expert Panel Recommendations – the new allergen reference doses for VITAL® program version 3.0, <https://bit.ly/2yE20ZQ> accessed on 9 December 2020.

Burks, A. W., Cockrell, G., Stanley, J. S., Helm, R. M., & Bannon, G. A. (1995). Recombinant peanut allergen Ara h I expression and IgE binding in patients with peanut hypersensitivity. *The Journal of Clinical Investigation, 96*(4), 1715–1721.

Chivers, C. E., Crozat, E., Chu, C., Moy, V. T., Sherratt, D. J., & Howarth, M. (2010). A streptavidin variant with slower biotin dissociation and increased mechanostability. *Nature Methods, 7*(5), 391–393.

Costa, J., Bavaro, S. L., Benedé, S., Diaz-Perales, A., Bueno-Diaz, C., Gelencser, E., Klueber, J., Larré, C., Lozano-Ojalve, D., & Lupi, R. (2020). Are physicochemical properties shaping the allergenic potency of plant allergens? *Clinical Reviews in Allergy & Immunology*, 1–27.

Crotty, M. P., & Taylor, S. L. (2010). Risks associated with foods having advisory milk labeling. *Journal of Allergy and Clinical Immunology, 125*(4), 935–937.

Du Toit, G., Sampson, H. A., Plaut, M., Burks, A. W., Akdis, C. A., & Lack, G. (2018). Food allergy: Update on prevention and tolerance. *Journal of Allergy and Clinical Immunology, 141*(1), 30–40.

Gezer, P. G., Liu, G. L., & Kokini, J. L. (2016). Development of a biodegradable sensor platform from gold coated zein nanophotonic films to detect peanut allergen, Ara h1, using surface enhanced raman spectroscopy. *Talanta, 150*, 224–232.

Goliáš, J., Humlová, Z., Halada, P., Hábová, V., Janatková, I., & Tučková, L. (2013). Identification of rice proteins recognized by the IgE antibodies of patients with food allergies. *Journal of Agricultural and Food Chemistry, 61*(37), 8851–8860.

Hahn, J., Kim, E., Han, H., & Choi, Y. J. (2020). Development of a portable lab-on-a-valve device for making primary diagnoses based on gold-nanoparticle aggregation induced by a switchable linker. *RSC Advances, 10*(52), 31243–31250.

Hahn, J., Kim, E., You, Y. S., Gunasekaran, S., Lim, S., & Choi, Y. J. (2017). A switchable linker-based immunoassay for ultrasensitive visible detection of salmonella in tomatoes. *Journal of Food Science, 82*(10), 2321–2328.

Holzhauser, T., Johnson, P., Hindley, J. P., O'Connor, G., Chan, C.-H., Costa, J., … Flanagan, S. D. (2020). Are current analytical methods suitable to verify VITAL® 2.0/3.0 allergen reference doses for EU allergens in foods? *Food and Chemical Toxicology, 145*, Article 111709.

Huang, C.-C., Huang, Y.-F., Cao, Z., Tan, W., & Chang, H.-T. (2005). Aptamer-modified gold nanoparticles for colorimetric determination of platelet-derived growth factors and their receptors. *Analytical Chemistry, 77*(17), 5735–5741.

Huang, Y., Bell, M. C., & Suni, I. I. (2008). Impedance biosensor for peanut protein Ara h 1. *Analytical Chemistry, 80*(23), 9157–9161.

Jayasena, S., Koppelman, S. J., Nayak, B., Taylor, S. L., & Baumert, J. L. (2019). Comparison of recovery and immunochemical detection of peanut proteins from differentially roasted peanut flour using ELISA. *Food Chemistry, 292*, 32–38.

Keum, E.-H., Lee, S.-I., & Oh, S.-S. (2006). Effect of enzymatic hydrolysis of 7S globulin, a soybean protein, on its allergenicity and identification of its allergenic hydrolyzed fragments using SDS-PAGE. *Food Science and Biotechnology, 15*(1), 128–132.

Lim, S., Koo, O. K., You, Y. S., Lee, Y. E., Kim, M.-S., Chang, P.-S., … Gunasekaran, S. (2012). Enhancing nanoparticle-based visible detection by controlling the extent of aggregation. *Scientific Reports, 2*(1). https://doi.org/10.1038/srep00456.

Liu, C., Wang, H., Cui, Z., He, X., Wang, X., Zeng, X., & Ma, H. (2007). Optimization of extraction and isolation for 11S and 7S globulins of soybean seed storage protein. *Food Chemistry, 102*(4), 1310–1316.

Mir, M. U. H., Maurya, J. K., Ali, S., Ubaid-ullah, S., Khan, A. B., & Patel, R. (2014). Molecular interaction of cationic gemini surfactant with bovine serum albumin: A spectroscopic and molecular docking study. *Process Biochemistry, 49*(4), 623–630.

Miyazaki, A., Watanabe, S., Ogata, K., Nagatomi, Y., Kokutani, R., Minegishi, Y., … Hirao, T. (2019). Real-time PCR detection methods for food allergens (wheat, buckwheat, and peanuts) using reference plasmids. *Journal of Agricultural and Food Chemistry, 67*(19), 5680–5686.

Montserrat, M., Sanz, D., Juan, T., Herrero, A., Sánchez, L., Calvo, M., & Pérez, M. D. (2015). Detection of peanut (Arachis hypogaea) allergens in processed foods by immunoassay: Influence of selected target protein and ELISA format applied. *Food Control, 54*, 300–307.

Ng, E., Nadeau, K. C., & Wang, S. X. (2016). Giant magnetoresistive sensor array for sensitive and specific multiplexed food allergen detection. *Biosensors and Bioelectronics, 80*, 359–365.

Palladino, C., & Breiteneder, H. (2018). Peanut allergens. *Molecular Immunology, 100*, 58–70.

Pavlov, V., Xiao, Y.i., Shlyahovsky, B., & Willner, I. (2004). Aptamer-functionalized Au nanoparticles for the amplified optical detection of thrombin. *Journal of the American Chemical Society, 126*(38), 11768–11769.

Puente-Lelievre, C., & Eischeid, A. C. (2018). Development and evaluation of a real-time PCR multiplex assay for the detection of allergenic peanut using chloroplast DNA markers. *Journal of Agricultural and Food Chemistry, 66*(32), 8623–8629.

Remington, B. C., Baumert, J. L., Blom, W. M., Houben, G. F., Taylor, S. L., & Kruizinga, A. G. (2015). Unintended allergens in precautionary labelled and unlabelled products pose significant risks to UK allergic consumers. *Allergy, 70*(7), 813–819.

Remington, B. C., Westerhout, J., Meima, M. Y., Blom, W. M., Kruizinga, A. G., Wheeler, M. W., … Baumert, J. L. (2020). Updated population minimal eliciting dose distributions for use in risk assessment of 14 priority food allergens. *Food and Chemical Toxicology, 139*, 111259. https://doi.org/10.1016/j.fct.2020.111259.

Rizzi, C., Zoccatelli, G., Simonato, B., Fratea, C., & Mainente, F. (2017). The food allergy risk management in the EU labelling legislation. *Journal of Agricultural and Environmental Ethics, 30*(2), 275–285.

Sendroiu, I. E., Mertens, S. F., & Schiffrin, D. J. (2006). Plasmon interactions between gold nanoparticles in aqueous solution with controlled spatial separation. *Physical Chemistry Chemical Physics, 8*(12), 1430–1436.

Sheu, S.-C., Tsou, P.-C., Lien, Y.-Y., & Lee, M.-S. (2018). Development of loop-mediated isothermal amplification (LAMP) assays for the rapid detection of allergic peanut in processed food. *Food Chemistry, 257*, 67–74.

Shoji, M., Adachi, R., & Akiyama, H. (2018). Japanese food allergen labeling regulation: An update. *Journal of AOAC International, 101*(1), 8–13.

Singh, H., Cantoria, M. J., Malave, P., Saputra, D., & Maleki, S. (2016). Standardization of RP-HPLC methods for the detection of the major peanut allergens Ara h 1, Ara h 2 and Ara h 3. *Food Chemistry, 194*, 383–390.

Sobhan, A., Oh, J.-H., Park, M.-K., Kim, S. W., Park, C., & Lee, J. (2018). Assessment of peanut allergen Ara h1 in processed foods using a SWCNTs-based nanobiosensor. *Bioscience, Biotechnology, and Biochemistry, 82*(7), 1134–1142.

van Boxtel, E. L., van Beers, M. M. C., Koppelman, S. J., van den Broek, L. A. M., & Gruppen, H. (2006). Allergen Ara h 1 occurs in peanuts as a large oligomer rather than as a trimer. *Journal of Agricultural and Food Chemistry, 54*(19), 7180–7186.

Walczyk, N. E., Smith, P. M. C., Tovey, E. R., & Roberts, T. H. (2017). Peanut protein extraction conditions strongly influence yield of allergens Ara h 1 and 2 and sensitivity of immunoassays. *Food Chemistry, 221*, 335–344.

You, Y., Lim, S., Hahn, J., Choi, Y. J., & Gunasekaran, S. (2018). Bifunctional linker-based immunosensing for rapid and visible detection of bacteria in real matrices. *Biosensors and Bioelectronics, 100*, 389–395.

Zhang, J., Hong, Y., Cai, Z., Huang, B., Wang, J., & Ren, Y. (2019). Simultaneous determination of major peanut allergens Ara h1 and Ara h2 in baked foodstuffs based on their signature peptides using ultra-performance liquid chromatography coupled to tandem mass spectrometry. *Analytical Methods, 11*(12), 1689–1696.

Zhang, M., Wu, P., Wu, J., Ping, J., & Wu, J. (2019). Advanced DNA-based methods for the detection of peanut allergens in processed food. *TrAC Trends in Analytical Chemistry, 114*, 278–292.